Rwanda Journal of Engineering, Science, Technology and Environment, Volume 7, Issue 1, Month 2025
eISSN: 2617-233X — print ISSN: 2617-2321

On $1+3$ covariant perturbation with chaplygin-stiff fluid system in modified Gauss-Bonnet gravity

Joseph Ntahompagaze[1], Fidele Twagirayezu[1], Abraham Ayirwanda[1], Albert Munyeshyaka[2], Solange Mukeshimana[3], Leon Fidele Ruganzu Uwimbabazi[3] and Justine Dushimirimana[3]

[1] *University of Rwanda, College of Science and Technology, Department of Physics, Kigali, Rwanda*

[2] *Mbarara University of Science and Technology, Department of Physics, Mbarara, Uganda*

[3] *University of Rwanda, College of Science and Technology, Department of Mathematics, College of Science and Technology, Kigali, Rwanda*

Correspondence: j.ntahompagaze@ur.ac.rw or ntahompagazej@gmail.com

Abstract

The early stage of the evolution of the universe, when taken along with the recent observations that the current universe is dominated by dark energy, leads to at least a potential problem that modern cosmology must address. Cosmology still lacks a model to deal with the observed current cosmic acceleration. In this paper, a framework is proposed to address the current accelerated expansion of the universe via large scale structure formation. In this regards, we investigate cosmological perturbations of modified Gauss-Bonnet ($f(G)$) gravity in the presence of a stiff fluid and two different forms of chaplygin gas model, using the $1+3$ covariant formalism. Gradient variables of respective fluids were defined to obtain the energy overdensity perturbation equations in redshift space, responsible for large scale structure formation. Using a particular functional form of $f(G)$ model, together with two different forms of chaplygin gas, the perturbation equations were solved separately to study the growth of energy overdensity contrast with redshift. The numerical results for both considered forms of chaplygin gas models show that the energy overdensity contrast decays with redshift which might enhance the large structure formation scenario.

Keywords: Perturbations; stiff fluid; cosmic acceleration; Gauss-Bonnet gravity; chaplygin gas

1 Introduction

In recent years, a number of cosmological observations have provided an increasing precise picture of the accelerated expansion of the universe. The baryon density has been estimated roughly at 5 percent of the critical density, as earlier estimate from the Big Bang Nucleosynthesis (BBN) [1], provided a confirmation through the Cosmic Microwave Background (CMB) observations from WMAP [2]. Additionally, a number of evidences from modern sources such as weak- [3] and strong- [4] lensing, large scale structure [5] as well as CMB have confirmed that another 23 percent energy density of the universe are in the form of dark matter as reveled from the rotational curves [6, 7]. In addition, different cosmological data, such as type I_a supernova [8], the CMB, baryonic acoustic oscillations [9] and gamma ray bursts [10] have presented convincing evidence that about 27 percent of the energy density of the universe forms an exotic, negative pressure component called dark energy.

Although the existence of all those components is reasonably well established, to solve the problems of dark matter and accelerating cosmic expansion driven by the dark energy, the existence of the other exotic fluid is not ruled out by the current data. For example, several models bring in the chaplygin gas [11, 12, 13]. The chaplygin gas acts as a cosmological fluid with an equation of state of the form $p_{chp} = -\frac{A}{\rho_{chp}^{\alpha}}$, where p_{chp} and ρ_{chp} are the pressure and energy density of the chaplygin gas, A and α are positive constants with $0 < \alpha < 1$. The chaplygin gas model acts as dark matter in the early universe whereas it acts as dark energy in the late-times of the universe. This model has been extended to its different variant forms such as original generalised chaplygin gas (OGG), generalised chaplygin gas (GCG), modified generalised chaplygin gas (MGCG), extended chaplygin gas (ECG) and generalised cosmic chaplygin gas (GCCG) [14, 15, 16].

Another exotic fluid is the stiff fluid, i.e, a fluid with an equation state parameter $w_s = \frac{p_s}{\rho_s} = 1$. This is the largest value of w consistent with causality [7], since the speed of sound of this fluid is equals to the speed of light. Such models were first studied by Zeldovich [17, 18], thereafter a variety of models, such as Kination [19], interacting dark matter [20], Horava-Lifshits [21, 22, 23] and non-singular cosmological models [24, 25, 26] have been proposed that produce a stiff cosmological fluid. Because the density of stiff fluid decays more rapidly than either radiation or matter , the effect of the stiff fluid on the expansion rate will be the largest at the early times [27, 28, 29] as previously discussed, the stiff fluids have usually quoted BBN limits on the expansion rate at fixed temperature and used these limits to constrain the density of the stiff fluid [7, 29].

An other approach to tackling the problem of dark matter and the current accelerated expansion of the universe is the use of modified theories of gravity such as $f(R)$, $f(T)$ and $f(G)$ to name but a few, where R, T and G are the Ricci scalar, torsion tensor and Gauss-Bonnet invariant parameter, respectively [30, 31, 32, 33]. In such kind of modified theories of gravity, the Einstein-Hilbert action is modified by adding a particular form of function of curvature terms. One of the advantages of these theories is that they can unify the early inflationary era to the late-time era of the universe in a way similar to the lambda Cold Dark matter (ΛCDM). Although the modified theories of gravity present numerous advantages in describing both the early and late time epochs of the universe, some of these models have been challenged to address different issues such as achieving a consistent description of neutron stars as discussed in [34], issue of dealing with the singularities problems [35], controlling matter instabilities as pointed out in [36] and satisfying solar system tests as pointed out in [35, 37]. But most of these challenges seems to be in absence in $f(G)$ models as pointed out in [38, 39, 40]. Therefore, there has been motivation in the use of such $f(G)$ gravity models. Different works have been attempted to combine $f(G)$ models with matter and scalar field or chaplygin gas models [41, 42, 43, 44, 16, 45, 46] to describe the early and late time epochs of the universe in a unified way. Our previous paper [47] considered a mixture of matter, chaplygin gas and Gauss-Bonnet fluids and found that the energy density perturbations decay with redshift in both long and short wavelength limits.

In this manuscript, we intend to consider a fluids-mixture of stiff fluid, chaplygin gas and Gauss-Bonnet fluid to investigate its implications on large scale structure formation. The best way to do this is through the use of $1+3$ covariant perturbations. Therefore, the study of linear cosmological perturbations is the main focus using the $1+3$ covariant formalism. There are two main approaches to study cosmological perturbations. The metric approach developed by Lifshitz [48], Bardeen [49] and Kodama and Sasaki [50] and the $1+3$ covariant formalism developed by Ehlers [51], Hawking [52], Olson [53] and, Ellis and Bruni [54]. The $1+3$ covariant formalism is advantageous due to for example its ability to present true physics and no unphysical gauge mode exist. It starts from theory and reduces to linearity in a particular background and non-linearities can be accommodated in such formalism [55]. Different works considered the $1+3$ covariant formalism to study the perturbations of the mixture of matter-chaplygin gas in $f(R)$ [56], matter-chaplygin gas in $f(T)$ gravity [57, 16, 58], matter-scalar field in $f(G)$ gravity [45]. Our recent work [47] considered the perturbations of matter chaplygin gas in $f(G)$ gravity. To our knowledge, there is no work in the literature that considered the cosmological perturbations of the stiff fluid-chaplygin gas-Gauss-Bonnet fluid mixture using the $1+3$ covariant formalism. Thus, this work intend to fill this important gap using such covariant approach. In so doing, we define gradient variables of involved fluids to derive linear perturbation equations. After obtaining the energy density perturbation equations in redshift space and considering a particular functional form of $f(G)$ model and different forms of chaplygin gas for pedagogical purpose, we present the numerical results and discuss their implications on both long and short-wavelength modes as far as large structure formation is concerned.

The rest of this paper is organised as follows: in Sect. 2, a review of background field equations and mathematical framework is presented; in Sect. 3, we present the $1+3$ covariant formalism in the context of $f(G)$ gravity, whereas in Sect. 4, we present, analyse the perturbation equations for matter fluctuations for both GR and the considered fluids mixture then discuss the results. Section 5 gives closing remarks.

2 Background field equations and mathematical framework

In this section, mathematical aspect is presented to describe the cosmic evolution. In this regard, vector and scalar gradient variables of individual fluid are defined in order to get the perturbation equations. First, On the large scale structure of the universe, the homogeneous and isotropic assumptions imply that the current universe is close to a flat geometry with radius of curvature R, same at every point in space and that the universe expansion has to be the same at every space with the scale factor $a(t)$. The relationship betwween curvature and matter content of the universe is given by the Einstein's equation represented as

$$G_{\mu\nu} \equiv R_{\mu\nu} - \frac{1}{2} g_{\mu\nu} R = 8\pi G_N T_{\mu\nu}, \tag{1}$$

where $G_{\mu\nu}$ is the Einstein tensor, $R_{\mu\nu}$, $R = g^{\mu\nu}R_{\mu\nu}$, $T_{\mu\nu}$ and G_N are Ricci tensor, Ricci scalar, energy momentum tensor and Newton gravitational constant respectively and $g^{\mu\nu}$ is the metric tensor. For a perfect fluid, the energy momentum tensor is given by

$$T_{\mu\nu} = (\rho + p)u^\mu u^\nu + p g^{\mu\nu}, \tag{2}$$

where, ρ and p are the energy density and isotropic pressure respectively and u^μ is the 4-velocity. Throughout this work, we shall assume that the geometrical background corresponds to that of a flat Friedman-Robert-Walker (FRW) metric, so that the line element is presented as

$$ds^2 = -dt^2 + a^2(t)\left(dx^2 + dy^2 + dz^2\right), \tag{3}$$

where $a(t)$ is the scale factor of the Universe. The metric tensor has the form

$$g_{\mu\nu} = diag(-1, a^2(t), a^2(t), a^2(t))$$

and for the flat metric, the curvature terms, which are Ricci scalar R and the Gauss-Bonnet invariant G are given by

$$R = 6\Big(2H^2 + \dot{H}\Big), \tag{4}$$

$$G = 24H^2\Big(H^2 + \dot{H}\Big), \tag{5}$$

where $H = \frac{\dot{a}}{a}$ is the Hubble parameter. The dot describes differentiation with respect to cosmic time t. For the metric of the form eq. (3) and considering a perfect fluid in a flat goemetry, the Friedmann, acceleration and the continuity equations are represented as

$$H^2 \equiv \left(\frac{\dot{a}}{a}\right)^2 = \frac{8\pi G_N \rho}{3}, \tag{6}$$

$$\dot{H} = -4\pi G_N(\rho + p), \tag{7}$$

$$\frac{\ddot{a}}{a} = \frac{-4\pi G_N}{3}(\rho + p), \tag{8}$$

$$\dot{\rho} + 3H\rho(1 + w) = 0, \tag{9}$$

where H is the Hubble parameter. The eq. (6) tells us that the universe containing matter has to be dynamically evolving. Knowing that the critical density of matter is given by $\rho_c \equiv \frac{3H^2}{8\pi G_N}$ and the density parameter $\Omega_i = \frac{\rho_i}{\rho_c}$, eq. (6) can be rewritten as

$$\sum_i \Omega_i = 1, \tag{10}$$

where Ω_i is the density parameter of the matter species present in the universe. For a barotropic perfect fluid with an equation of state parameter given by $w = \frac{p}{\rho}$, and from eq. (6) and eq. (7), one gets [59]

$$H = \frac{2}{3(1 + w)(t - t_0)}, \tag{11}$$

$$a(t) \propto (t - t_0)^{\frac{2}{3(1+w)}}, \tag{12}$$

$$\rho \propto a^{-3(1+w)}, \tag{13}$$

whereby for a universe dominated by a dust with an equation of state parameter ($w = 0$), or radiation ($w = \frac{1}{3}$), yields $a(t) \propto (t - t_0)^{\frac{2}{3}}$, $\rho \propto a^{-3}$ and $a(t) \propto (t - t_0)^{\frac{1}{2}}$, $\rho \propto a^{-4}$ respectively, leading to a decelerated expansion of the universe as presented in eq. (8). The accelerated expansion ($a(t) > 0$) occurs for $w < -\frac{1}{3}$. In order to include dark energy terms responsible for the accelerated expansion of the Universe, the consideration of stiff fluid, modified-Chaplygin gas and Gauss-Bonnet fluids was done. Let us define the total energy density and isotropic pressure in the modified Gauss-Bonnet gravity as

$$\rho_t = 3H^2, \tag{14}$$

$$p_t = -(3H^2 + 2\dot{H}), \tag{15}$$

where

$$\rho_t = \rho_s + \rho_{chp} + \rho_G, \tag{16}$$
$$p_t = p_s + p_{chp} + p_G, \tag{17}$$

and ρ_s and p_s denote the energy density and pressure of the stiff fluid with an equation state parameter equals to unity ($w_s = 1$). Considering an $f(G)$ model given by $f(G) = cG^\beta$ [60, 35] together with generalised modified Chaplygin gas given by $p_{ch} = B\rho_{chap} - (1+B)\frac{A}{(\rho_{ch})^\alpha}$ and modified chaplygin gas given by $p_{ch} = A\rho - \frac{B}{\rho^\alpha}$, with A,B constants and $0 < \alpha < 1$) [16], one can show that modified gravity can lead to quite rich and realistic cosmological dynamics [33]. The pressures and energy densities are given by

$$\rho_G = \frac{1}{2}\Big(f'G - f\Big) - 24f''H^3\dot{G}, \tag{18}$$
$$p_G = \frac{1}{2}(f - f'G) + \frac{G\dot{G}}{3H}f'' + 4H^2\ddot{G}f'' + 4H^2\dot{G}^2f''', \tag{19}$$
$$\rho_{ch} = \Big[A + ca^{-3(1+\alpha)(1+B)}\Big]^{\frac{1}{1+\alpha}}, \tag{20}$$
$$p_{ch} = B\rho_{chap} - (1+B)\frac{A}{(\rho_{ch})^\alpha}, \tag{21}$$
$$\rho_s \propto a^{-6}. \tag{22}$$

A convenient way for the investigation of the dynamics of late-time universe is to replace cosmic time with redshift as dynamical parameter. Redshift transformation technique is conducted basing on the following definitions as pointed out in [45, 58, 61] .

$$a = \frac{1}{1+z}, \tag{23}$$
$$\dot{f} = -(1+z)Hf', \tag{24}$$
$$\ddot{f} = (1+z)^2H\Big(\frac{dH}{dz}\frac{df}{dz} + H\frac{d^2f}{dz^2}\Big) + (1+z)H^2\frac{df}{dz}, \tag{25}$$

where the current scale factor is considered to be equals to unity for simplicity. Hence, the present value of cosmological redshift is set to zero. According to the mentioned transformation technique, the involved time derivatives which are the energy density and pressure of Gauss-Bonnet fluids (eq. (18) and eq. (19)), the energy density, isotropic pressure of the modified chaplygin gas (eq. (20) and eq. (21)) and eq. (22), can be expressed in terms of redshift as

$$\rho_G = \frac{1}{2}c(\beta-1)G^\beta\Big[1 + 48\beta(1+z)\frac{G'H^4}{G^2}\Big], \tag{26}$$
$$\begin{aligned} p_G = \frac{1}{2}c(\beta-1)G^\beta\Big[-\frac{2\beta(1+z)G'}{3G} - 1 + \frac{8H^2\beta}{G^2}\bigg(\Big((1+z)H' + H\Big)(1+z)HG' \\ +(1+z)^2H^2G'' + \frac{(\beta-2)\Big((1+z)HG'\Big)^2}{G}\bigg)\Big], \end{aligned} \tag{27}$$
$$\rho_{ch} = \Big[A + c(1+z)^{3(1+\alpha)(1+B)}\Big]^{\frac{1}{1+\alpha}}, \tag{28}$$
$$p_{ch} = B\rho_{chap} - (1+B)\frac{A}{(\rho_{ch})^\alpha}, \tag{29}$$
$$\rho_s = \rho_{0s}(1+z)^6, \tag{30}$$

where the prime denotes the differentiation with respect to redshift. Eq. (7) represents a more generalised version of the modified chaplygin gas model presented in [56, 16], with the energy density (eq. 6) resulted from eq. (7) so that the equation corresponding to the Friedman equation is modified as

$$3H^2 = \frac{1}{2}c(\beta-1)G^\beta\Big[1+48\beta(1+z)\frac{G'H^4}{G^2}\Big] + \rho_s + \Big[A+(1+z)^{3(1+\alpha)(1+B)}\Big]^{\frac{1}{1+\alpha}}\ , \tag{31}$$
$$G = 24H^3(H-(1+z)H')\ , \tag{32}$$
$$R = 6H(2H-(1+z)H')\ , \tag{33}$$

where A, B, α and C are arbitrary constants, $H = \frac{\dot{a}}{a}$ is the Hubble parameter and a is the scale factor. The dark energy density which involves all the geometrical terms appearing on the right hand side of Friedman equation and the pressure orginating from dark energy are given by

$$\rho_{de} = \frac{1}{2}c(\beta-1)G^\beta\Big[1+48\beta(1+z)\frac{G'H^4}{G^2}\Big] + \Big[A+(1+z)^{3(1+\alpha)(1+B)}\Big]^{\frac{1}{1+\alpha}} \tag{34}$$
$$p_{de} = \frac{1}{2}c(\beta-1)G^\beta\Big[-\frac{2\beta(1+z)G'}{3G} - 1 + \frac{8H^2\beta}{G^2}\Big(\Big((1+z)H'+H\Big)(1+z)HG'$$
$$+(1+z)^2H^2G'' + \frac{(\beta-2)\Big((1+z)HG'\Big)^2}{G}\Big)\Big] + B\rho_{chap} - (1+B)\frac{A}{(\rho_{ch})^\alpha}. \tag{35}$$

Instead of cosmological constant, now a function of redshift appears in both equations, and the dark energy also behaves a perfect fluid, since Hubble and matter components are also considered as perfect fluids. Therefore the continuity equation for dark energy has the form

$$\dot{\rho_{de}} + 3H(\rho_{de}+p_{de}) = 0. \tag{36}$$

where there is no coupling between matter and dark energy present. Next section present the $1+3$ covariant formalism which is useful in the construction of perturbation equations.

3 Description of the $1+3$ covariant formalism in the context of $f(G)$ gravity

The $1+3$ covariant decomposition is a framework used in describing the linear evolution of the cosmological perturbations [62]. In this approach, a fundamental observer divides space-time into hyper-surfaces and a perpendicular 4-velocity field vector, where $1+3$ indicates the number of dimensions involved in each slice [63]. That is to mean that manifold geometry of the GR is described in four dimensional space (ie,. time and space). One of the importance of the $1+3$ covariant approach is to identify a set of covariant variables which describe the inhomogeneity and anisotropy of the universe [64]. In this context, we define a four-vector coordinates function of cosmological time ($x^\mu = x^\mu(\tau)$) that labels the co-moving distance along a world-line and the corresponding velocity given by:

$$u^\mu = \frac{dx^\mu}{d\tau} \tag{37}$$

The projection tensor, $h_{\alpha\beta}$ into the three dimensional and orthogonal to u^μ, satisfy the following condition:

$$h_{\alpha\beta} = g_{\alpha\beta} + u_\alpha u_\beta \Rightarrow h^\alpha_\beta h^\beta_\gamma = h^\alpha_\gamma, \tag{38}$$
$$h^\alpha_\alpha = 3, h_{\alpha\beta}u^\beta = 0. \tag{39}$$

The covariant derivative of the four-velocitiy in terms of its kinematic quantities [65] is given by:

$$\tilde{\nabla}_a u_b = \frac{1}{3}h_{ab}\tilde{\theta} + \tilde{\sigma}_{ab} + \tilde{\omega}_{ab} - u_a\dot{\tilde{u}}_b, \quad (40)$$

where θ, $\tilde{\sigma}_{ab}$, $\tilde{\omega}_{ab}$, $\dot{\tilde{u}}_b$, are: the volume expansion, shear tensor, vorticity tensor and four-acceleration respectively. The Hubble parameter is related to θ as $\theta = 3H$. Assume the fluids in our consideration are irrotational (ie.,$\tilde{\omega}_{ab} = 0$) and shear-free (i.e $\tilde{\sigma}_{ab} = 0$), the rate of expansion is given by the Raychaudhuri and conservation equations as:

$$\dot{\theta} = -\frac{\theta^2}{3} - \frac{1}{2}(\rho_t + 3p_t) + \tilde{\nabla}^a\dot{u}_a, \quad (41)$$

$$\dot{\rho}_t = -\theta(\rho_t + p_t), \quad (42)$$

$$\tilde{\nabla}_a p_t - (\rho_t + p_t)\dot{u}_a = 0. \quad (43)$$

Eq. (41)–(43) are useful for constructing perturbation equations from the gradient variables of different fluids in the next subsection

3.1 General fluids description and perturbation equations

In this part, we assume a non-interacting stiff fluid with both generalized and modified chaplygin gas and Gauss-Bonnet fluids in the entire Universe where the growth of the energy overdensity fluctuations contribute to the large scale structure formation. It is currently a well known fact that the universe is not perfectly smooth, but made of large scale structures such as galaxies, clusters, voids to name but a few, believed to be seeded from primordial fluctuations. Cosmological perturbations theory provides the mechanism to explain how these primordial fluctuations grow and form the large scale structures we see today in the universe [55]. The covariant formalism describes space-time through covariantly defined variables with respect to the frame such as 1+3 space-time decomposition technique which helps in describing physics and geometry using tensor quantities and relations valid in all coordinate systems. We start by defining the covariant and Gauge-Invariant gradient variables that describe the stiff fluid, chaplygin gas, Gauss-Bonnet energy densities and expansion, as per the 1 + 3 covariant perturbation formalism [48, 62, 66, 55]. We consider an homogenous and expanding (FRW) cosmological background to define the spatial gradient of the Gauge invariant variables such as $D^s_a = \frac{a\tilde{\nabla}^a\rho_s}{\rho_s}, Z_a = a\tilde{\nabla}^a\theta, D^{ch}_a = \frac{a\tilde{\nabla}_a\rho_{ch}}{\rho_{ch}}, D^G_a = \frac{a\tilde{\nabla}_a\rho_G}{\rho_G}, \mathcal{G}_a = a\tilde{\nabla}_a G, \mathsf{G}_a = a\tilde{\nabla}_a\dot{G}$. The subscripts s, G and chp stand for stiff fluid, Gauss-Bonnet fluid, Chaplygin gas fluid contributions, respectively. The scalar gradient variables can be extracted from the defined vector gradient variables using local decomposition and scalar decomposition techniques and presented as

$$\Delta^s = \tilde{\nabla}^a\Big(\frac{a\tilde{\nabla}^a\rho_s}{\rho_s}\Big), \tag{44}$$

$$Z = \tilde{\nabla}^a\Big(a\tilde{\nabla}^a\theta\Big), \tag{45}$$

$$\Delta^{ch} = \tilde{\nabla}^a\Big(\frac{a\tilde{\nabla}_a\rho_{ch}}{\rho_{ch}}\Big)\ , \tag{46}$$

$$\Delta^G = \tilde{\nabla}^a\Big(\frac{a\tilde{\nabla}_a\rho_G}{\rho_G}\Big), \tag{47}$$

$$\mathcal{G} = \tilde{\nabla}^a\Big(a\tilde{\nabla}_a G\Big), \tag{48}$$

$$\mathsf{G} = \tilde{\nabla}^a\Big(a\tilde{\nabla}_a\dot{G}\Big)\ . \tag{49}$$

We apply time derivative to eq. (44) through to eq. (49) to develop a system of cosmological perturbation equations in the context of modified $f(G)$ gravity for two different forms of chaplygin-gas model, namely the generalised version of modified chaplygin gas and the modified chaplygin gas [16, 56]. Considering the first case of the generalised version of modified chaplygin gas, from eq. (20), the vector term $a\tilde{\triangledown}_a w_{ch}$ provides its scalar part as

$$a\tilde{\triangledown}_a w_{ch} = \Big((1+B)(1+\alpha)A\Big)\Delta_{ch}, \tag{50}$$

and the 4-acceleration is given by

$$\dot{u}_a = -\frac{\tilde{\nabla}^a p_t}{\rho_t + p_t}, \tag{51}$$

$$a\dot{u}_a = -\frac{1}{(1+w_t)\rho_t}\Big[\rho_m D^a_m + w_{chp}\rho_{chp}D^a_{chp} + a\rho_{chp}\tilde{\nabla}^a w_{chp} + \tilde{\nabla}^a p_G\Big]\ . \tag{52}$$

In the following section, we present the perturbation equations for two different cases of the considered chaplygin gas with their respective numerical solutions.

4 Results and Discussion

In this section, we consider two different forms of chaplygin gas model to check its implications on large scale structure formation.

4.1 Perturbation equations for generalised modified chaplygin gas model

Time derivative of eq. (44)–(49) and the application of scalar and harmonic decomposition techniques yield the linear scalar perturbation equations for the stiff fluid, generalised modified chaplygin gas and Gauss-Bonnet energy densities. Using a functional form of $f(G)$ model given by $f(G) = cG^{\beta}$, the linear perturbation equations obtained are represented in redshift space as

$$
\begin{aligned}
\Delta_s' &= \frac{1}{(1+z)H}\left(2+\frac{2}{(1+w_t)\rho_t}\frac{G\big(-(1+z)H)\big)G'}{\theta^2}\right)Z - \frac{1}{(1+z)H}\frac{2}{(1+w_t)}\frac{\rho_s}{\rho_t}\theta\Delta_s\\
&+\frac{1}{(1+z)H}(1+(1+B)(\alpha+1)A)\frac{2}{(1+w_t)\rho_t}w_{chp}\rho_{chp}\Delta_{chp}+\frac{2}{(1+w_t)\rho_t}\frac{c\beta(\beta-1)G^{\beta-1}}{\theta}\mathsf{G}\\
&-\frac{1}{(1+z)H}\frac{2}{(1+w_t)\rho_t}\Big(\frac{1}{2}(G-c\beta^2G^{\beta})(1+z)HG'c\beta(\beta-1)(\beta-2)G^{\beta-3}\\
&-(1+z)HG'c\beta(\beta-1)G^{\beta-4}\Big)\mathcal{G}, \qquad (53)\\
Z' &= -\frac{1}{(1+z)H}\Big[-\frac{1}{2}\Big(4\rho_s-\big(\frac{1}{3}\theta^2+\frac{1}{2}(1+3w_t)\rho_t\big)\Big)\frac{\rho_s}{(1+w_t)\rho_t}-\frac{\rho_s}{(1+w_t)\rho_t}\frac{k^2}{a^2}\Big]\Delta_s\\
&-\frac{1}{(1+z)H}\Big[\frac{\rho_{ch}\Big(w_{ch}+(1+B)(1+\alpha)A\Big)}{(1+w_t)\rho_t}\Big(k^2+\frac{\theta^2}{3}+\frac{1}{2}(1+w_t)\rho_t\Big)+\Big(2+3w_{ch}\Big)\rho_{ch}\Big]\Delta_{chp}\\
&-\frac{1}{(1+z)H}\Big[1-3c\beta(\beta-1)G^{\beta-2}-12H^3b_1c\beta(\beta-1)(\beta-2)(\beta-3)G^{\beta-4}\\
&+12H\Big(H(b_2c(\beta)(\beta-1)(\beta-2)G^{\beta-3}+\frac{b_3}{b_1}c(\beta)(\beta-1)G^{\beta-2}+b_1^2c(\beta)(\beta-1)(\beta-2)(\beta-3)G^{\beta-4})\\
&+2H^3c(\beta)(\beta-1)G^{\beta-2}\Big)+\big(\frac{1}{3}\theta^2+\frac{1}{2}(1+3w_t)\rho_t\big)\frac{1}{(1+w_t)\rho_t}\Big(\frac{1}{2}(1-c(\beta)G^{\beta-1}-Gc(\beta)G^{\beta-1}\\
&-Gc(\beta)(\beta-1)G^{\beta-2})+Gb_1c(\beta)(\beta-1)(\beta-2)G^{\beta-3}+b_1c(\beta)(\beta-1)G^{\beta-4}\Big)\\
&-\frac{1}{(1+w_t)\rho_t}\frac{k^2}{a^2}\Big(\frac{1}{2}(1-c(\beta)G^{\beta-1}-c(\beta)(\beta-1)G^{\beta-1})+b_1c(\beta)(\beta-1)(\beta-2)G^{\beta-2}\\
&+b_1c(\beta)(\beta-1)G^{\beta-4}\Big)\Big]\mathcal{G}-\frac{1}{(1+z)H}\Big(24b_1c(\beta)(\beta-1)(\beta-2)G^{\beta-3}-12H^3c(\beta)(\beta-1)(\beta-2)G^{\beta-3}\\
&+\big(\frac{1}{3}\theta^2+\frac{1}{2}(1+3w_t)\rho_t\big)\frac{c(\beta)(\beta-1)G^{\beta-1}}{\theta(1+w_t)\rho_t}-\frac{1}{(1+w_t)\rho_t}\frac{k^2}{a^2}\frac{c(\beta)(\beta-1)G^{\beta-1}}{\theta}\Big)\mathbf{G}\\
&-\frac{1}{(1+z)H}\Big[8H\Big(c(\beta)(\beta-1)G^{\beta-2}b_2+c(\beta)(\beta-1)(\beta-2)G^{\beta-3}b_1^2+3Hc(\beta)G^{\beta-1}\\
&-\frac{3}{2}c(\beta)(\beta-1)(\beta-2)G^{\beta-3}Hb_1\Big)-\frac{2}{3}\theta-\big(\frac{1}{3}\theta^2+\frac{1}{2}(1+3w_t)\rho_t\big)\frac{Gb_1}{\theta^2(1+w_t)\rho_t}\\
&+\frac{k^2}{a^2(1+w_t)\rho_t}\frac{Gb_1}{\theta^2}\Big]Z, \qquad (54)
\end{aligned}
$$

$$\mathcal{G}' = -\frac{1}{(1+z)H}\Big(1-\frac{b_1c(\beta)(\beta-1)G^{\beta-1}}{(1+w_t)\rho_t\theta}\Big)\mathsf{G} - \frac{1}{(1+z)H}\frac{b_1^2 G}{(1+w_t)\rho_t\theta^2}Z$$
$$+\frac{1}{(1+z)H}\frac{b_1\rho_s\Delta_s}{(1+w_t)\rho_t} - \frac{1}{(1+z)H}\frac{b_1\rho_{ch}}{(1+w_t)\rho_t}\Big(w_{ch}+(1+B)(1+\alpha)A\Big)\Delta_{chp}$$
$$+\Big(\frac{1}{2(1+z)H}\frac{b_1}{(1+w_t)\rho_t}\Big(c(\beta)G^{\beta-1}+c(\beta)(\beta-1)G^{\beta-1}-1\Big)$$
$$+\frac{1}{2(1+z)H}\frac{b_1^2}{(1+w_t)\rho_t}\Big(c(\beta)(\beta-1)G^{\beta-1}+\frac{c(\beta)(\beta-1)G^{\beta-2}}{\theta^2}\Big)\Big)\mathcal{G}, \tag{55}$$

$$\mathsf{G}' = -\frac{1}{(1+z)H}\Big(\frac{b_3}{b_1}-\frac{b_1c(\beta)(\beta-1)G^{\beta-1}}{(1+w_t)\rho_t\theta}\Big)\mathsf{G} + \Big[\frac{1}{(1+z)H}\frac{b_2b_1G}{(1+w_t)\rho_t\theta^2}\Big]Z$$
$$+\Big[\frac{1}{(1+z)H}\frac{b_2}{(1+w_t)\rho_t}\rho_s\Big]\Delta_s - \Big[\frac{1}{(1+z)H}\frac{b_2\rho_{ch}}{(1+w_t)\rho_t}\Big(w_{ch}+(1+B)(1+\alpha)A\Big)\Big]\Delta_{ch}$$
$$-\frac{1}{(1+z)H}\Big[\frac{b_2}{2(1+w_t)\rho_t}(c(\beta)G^{\beta-1}+c(\beta)(\beta-1)G^{\beta-1}-1)-\frac{b_2b_1}{(1+w_t)\rho_t}(c(\beta)(\beta-1)G^{\beta-1}$$
$$+\frac{c(\beta)(\beta-1)G^{\beta-2}}{\theta^2})\Big]\mathcal{G} \tag{56}$$

$$\Delta'_G = -\frac{1}{(1+z)H}\Big[-\frac{4H\theta}{\rho_G}\Big(2Hb_1c(\beta)(\beta-1)(\beta-2)G^{\beta-3}+(2c_1-2H^2)c(\beta)(\beta-1)G^{\beta-2}\Big)$$
$$+\theta\Big(4H^2c(\beta)(\beta-1)G^{\beta-2}b_2+4H(2c_1-H^2)c(\beta)(\beta-1)G^{\beta-2}b_1\Big)\Big(\frac{c(\beta)(\beta-1)G^{\beta-1}}{\theta(1+w_t)\rho_t\rho_G}\Big)\Big]\mathsf{G}$$
$$-\frac{1}{(1+z)H}\Big[4H\Big(H(b_2c(\beta)(\beta-1)(\beta-2)G^{\beta-3}+\frac{c(\beta)(\beta-1)G^{\beta-2}b_2}{b_2}+b_2^2c(\beta)(\beta-1)(\beta-2)G^{\beta-3})$$
$$+(2c_1-H^2)c(\beta)(\beta-1)G^{\beta-2}\Big)+\theta\Big(4H^2(c(\beta)(\beta-1)G^{\beta-2}b_2+c(\beta)(\beta-1)(\beta-2)G^{\beta-3}b_1^2))$$
$$+4H(2c_1-H^2)c(\beta)(\beta-1)G^{\beta-2}b_1\Big(\frac{\frac{1}{2}+b_1c(\beta)(\beta-1)G^{\beta-1}+\frac{b_1c(\beta)(\beta-1)(\beta-2)G^{\beta-3}}{\theta^2}}{(1+w_t)\rho_t\rho_G}\Big)\Big]\mathcal{G}$$
$$-\frac{1}{3((1+z)H)\rho_G}\Big[\Big(2H(c(\beta)(\beta-1)G^{\beta-2}b_2+c(\beta)(\beta-1)(\beta-2)G^{\beta-3}b_1^2)$$
$$-8Hc(\beta)(\beta-1)G^{\beta-2}b_1(\frac{G}{12H^3}+3H)+(2c_1-H^2)c(\beta)(\beta-1)G^{\beta-2}b_1-3\Big(4H^2(c(\beta)(\beta-1)G^{\beta-2}b_2$$
$$+c(\beta)(\beta-1)(\beta-2)G^{\beta-3}b_1^2)+4H(2c_1-H^2)c(\beta)(\beta-1)G^{\beta-2}b_1\Big)+\theta(4H^2(c(\beta)(\beta-1)G^{\beta-2}b_2$$
$$+c(\beta)(\beta-1)(\beta-2)G^{\beta-3}b_1^2)-4H(2c_1-H^2)c(\beta)(\beta-1)G^{\beta-2}b_1)(\frac{Gb_1\theta^2}{(1+w_t)\rho_t\rho_G})\Big)$$
$$+3\theta(4H^2(c(\beta)(\beta-1)G^{\beta-2}b_2+c(\beta)(\beta-1)(\beta-2)G^{\beta-3}b_1^2)$$
$$+4H(2c_1-H^2)c(\beta)(\beta-1)G^{\beta-2}b_1)\Big(\frac{(1-(2+\beta)c(\beta)G^{\beta}b_1}{\theta^2(1+w_t)\rho_t}\Big)\Big]Z$$
$$-\frac{3}{(1+z)\rho_G}\Big(4H^2(c(\beta)(\beta-1)G^{\beta-2}b_2+c(\beta)(\beta-1)(\beta-2)G^{\beta-3}b_1^2)+4H(2c_1-H^2)f''b_1\Big)\Delta_G$$
$$-\frac{3}{(1+z)}\Big(-4H^2(c(\beta)(\beta-1)G^{\beta-2}b_2+c(\beta)(\beta-1)(\beta-2)G^{\beta-3}b_1^2)$$
$$+4H(2c_1-H^2)c(\beta)(\beta-1)G^{\beta-2}b_1\Big)\frac{\rho_s(1-c(\beta)G^{\beta-1}-c(\beta)(\beta-1)G^{\beta-1})}{(1+w_t\rho_t\rho_G)}\Delta_s$$
$$+\frac{3}{(1+z)}\Big(4H^2(c(\beta)(\beta-1)G^{\beta-2}b_2+c(\beta)(\beta-1)(\beta-2)G^{\beta-3}b_1^2)$$
$$+4H(2c_1-H^2)c(\beta)(\beta-1)G^{\beta-2}b_1\Big)\Big(\frac{w_{ch}\rho_{ch}}{(1+w_t)\rho_t\rho_G}\Big)\Big((1+B)(1+\alpha)A\Big)\Delta_{chp}, \tag{57}$$

$$\Delta_{ch}^{'} = \frac{1}{(1+z)H}[1+\frac{Gb_1}{\theta(1+w_t)\rho_t}](1+w_{ch})Z - \frac{1}{(1+z)H}\frac{\theta(1+w_{ch})}{(1+w_t)\rho_t}\rho_s\Delta_s$$
$$-\frac{3}{(1+z)}\Big[(1+\rho_{ch})\frac{(1+w_{ch})}{(1+w_t)\rho_t}w_{ch}\rho_{ch} - \Big(1+(1+B)(\alpha+1)A\Big)\theta\Big]\Delta_{ch}$$
$$-\frac{\theta(1+w_{ch})}{(1+z)(1+w_t)H\rho_t}\Big[\frac{1}{2}(1-c(\beta)G^{\beta-1}-c(\beta)(\beta-1)G^{\beta-1})+b_1c(\beta)(\beta-1)G^{\beta-1}$$
$$+\frac{b_1c(\beta)(\beta-1)(\beta-2)G^{\beta-3}}{\theta^2}\Big]\mathcal{G} - \frac{\theta(1+w_{ch})c(\beta)(\beta-1)G^{\beta-1}}{(1+z)(1+w_t)H\rho_t}\mathsf{G}\,, \tag{58}$$

where $k = \frac{2\pi a}{\lambda}$, k being the wave number and λ, the wavelength of perturbations. The equations eq. (53–58) represent the evolution of the energy density of the stiff fluid, the volume expansion, the Gauss-Bonnet fluid, Gauss-Bonnet momentum, the energy density resulting from the Gauss-Bonnet fluid and the energy density of the generalised modified chaplygin gas, respectively. The parameters b_1, b_2, b_3 represent the first, second and third derivatives of the Gauss-Bonnet parameter G, respectively. In GR limit, with normal form of matter, one can obtain a closed system of first-order perturbation equations which is easier to find the analytical solutions. However, the linear perturbation equations presented in this work (eq. (53)–(58)) are coupled system of first -order equations for the density fluctuations of stiff-, modified-chaplygin gas and Gauss-Bonnet fluids which are more complicated to find the analytical solutions. To numerically solve our perturbation equations, and check how the results compare with the GR or ΛCDM model, we have considered short wavelength ($\frac{k^2}{a^2H^2} \gg 1$) and long wavelength ($\frac{k^2}{a^2H^2} \ll 1$) limits of the perturbation to analyse the large scale structure implications of the numerical results using different initial conditions. In the following, we analyse the evolution of the perturbation equations in both long-wavelength and short-wavelength regimes by only considering that the universe is mainly dominated by stiff- generalised modified chaplygin gas-Gauss-Bonnet fluids mixture. First let us consider the case where the universe is mainly dominated by only stiff-fluid.

4.1.1 Matter density fluctuations in GR limits

In this part, we analyse the behavior of energy overdensity fluctuations for stiff fluid in GR limits for the case $f(G) = G$ and no contribution from any form of the considered chaplygin gas models. We also define the normalised energy density contrast as

$$\delta(z) = \frac{\Delta_s^k(z)}{\Delta(z_0)}, \tag{59}$$

where $\Delta(z_0)$ is the matter energy density at the initial redshift, hereafter $z_0 = 4$. If we assume that the Universe is dominated mainly by stiff fluid, the equation of state parameter becomes $w = 1$. Consequently eq. (53) through to eq. (58) reduce to

$$\Delta_s' = \frac{2}{(1+z)H}Z - \frac{3}{(1+z)}\Delta_s, \tag{60}$$
$$Z' = \frac{1}{2(1+z)H}\Big[\frac{\theta^2}{6} - \rho_s - \Big(1+z\Big)^2k^2\Big]\Delta_s' - \frac{2}{(1+z)}Z, \tag{61}$$

which (eq. (60)–(61)) admit the numerical solutions presented in figure. (1). In what follows, figure. (1) shows the evolution of the stiff fluid model in redshift space. As expected, figure.

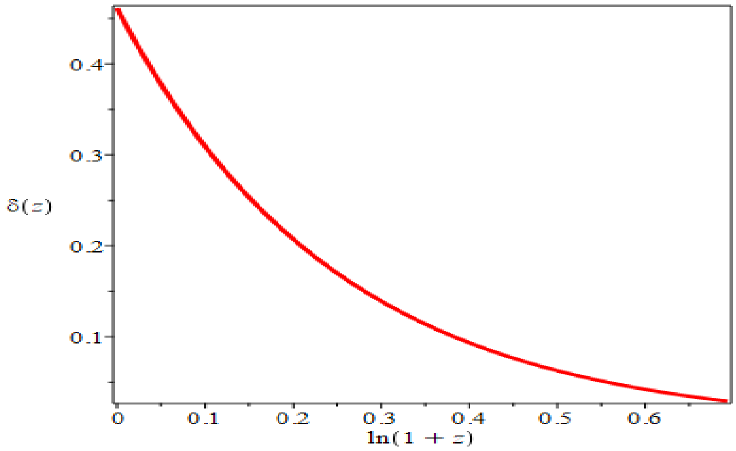

Figure 1: Plot of energy density contrast vs redshift of eq. (60) and eq. (61) using $k = 0.01$. During the numerical computation, we used the initial conditions $\Delta_s(z_{in} = 4) = 10^{-5}$ and $Z(z_{in} = 4) = 10^{-5}$. It is clear that Δ_s and Z couple, therefore once one gets the solution of Δ_s, it is possible to predict how the Z evolves. This plot shows that the energy density of the stiff fluid decays with redshift.

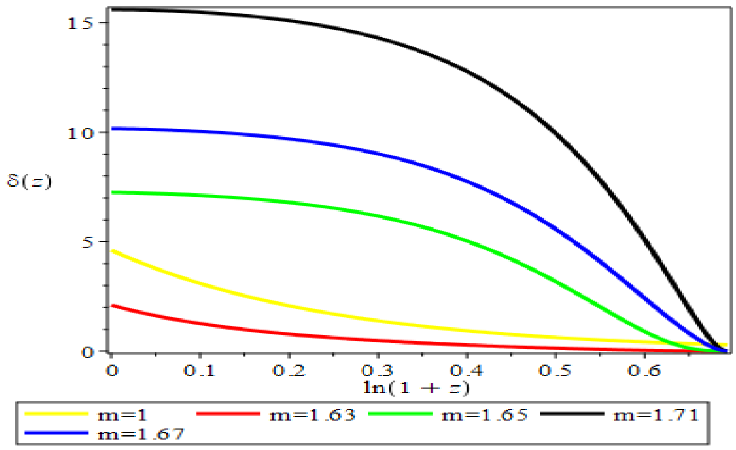

Figure 2: Plot of energy density contrast vs redshift of equations Eq. (53)–(Eq. 58), using $k = 0.000001$, long wavelength limit. During numerical integration, we considered different constant parameters to see whether there is any effect on the energy density contrast or not whereas $\Delta_s(z_{in} = 4) = 10^{-5}$, $Z(z_{in} = 4) = 10^{-5}$, $\mathcal{G}(z_{in} = 4) = 10^{-5}$, $\mathbf{G}(z_{in} = 4) = 10^{-5}$, $\Delta_{chp}(z_{in} = 4) = 10^{-5}$ were used as initial conditions. From the plots, for different parameter m, we depict that the energy overdensity contrast decay with redshift and as m changes, the behavior of the curves changes.

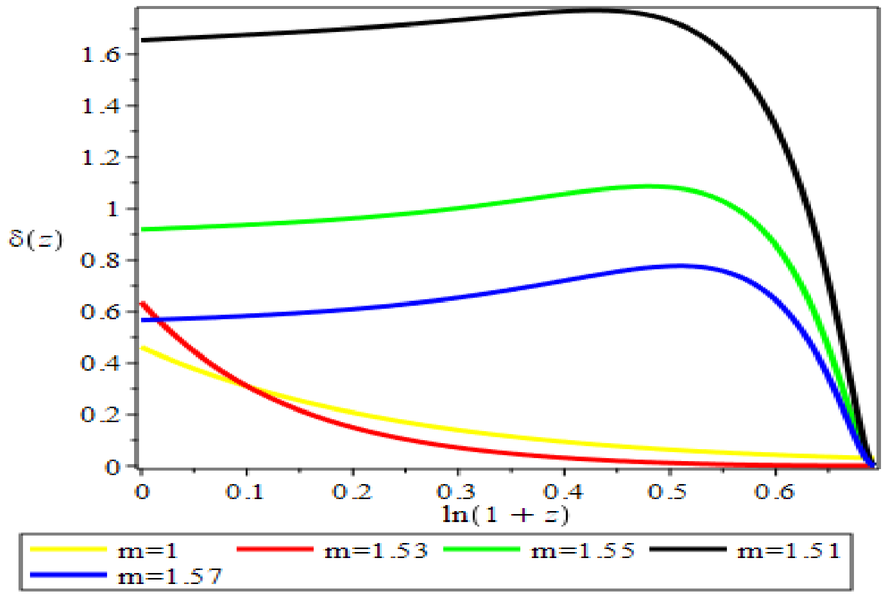

Figure 3: Plot of energy density contrast vs redshift of equations Eq. (53)–(Eq. 58), using $k = 0.01$ and $\alpha = 0.8$ in the long wavelength limit. During numerical integration, we considered different constant parameters to see whether there is any effect on the energy density contrast or not whereas $\Delta_s(z_{in} = 4) = 10^{-5}$, $Z(z_{in} = 4) = 10^{-5}$, $\mathcal{G}(z_{in} = 4) = 10^{-5}$, $\mathbf{G}(z_{in} = 4) = 10^{-5}$, $\Delta_{chp}(z_{in} = 4) = 10^{-5}$ were used as initial conditions. From the plots, for different parameter m, we depict that the energy overdensity contrast decay with redshift and as m changes, the behavior of the curves changes.

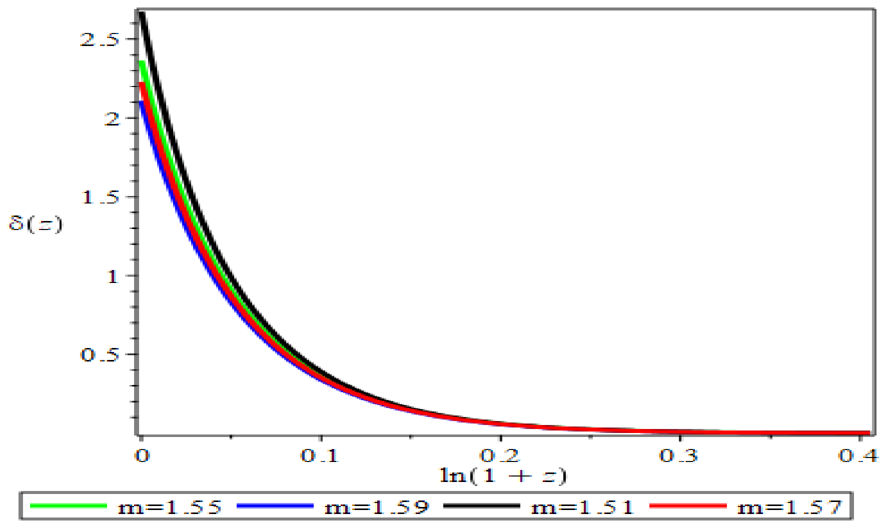

Figure 4: Plot of energy density contrast vs redshift of equations Eq. (53)–(Eq. 58), using $k = 100$, short wavelength limit. During numerical integration, we considered different constant parameters to see whether there is any effect on the energy density contrast or not whereas $\Delta_s(z_{in} = 4) = 10^{-5}$, $Z(z_{in} = 4) = 10^{-5}$, $\mathcal{G}(z_{in} = 4) = 10^{-5}$, $\mathbf{G}(z_{in} = 4) = 10^{-5}$, $\Delta_{chp}(z_{in} = 4) = 10^{-5}$ were used as initial conditions. From the plots, for different parameter m, we depict that the energy overdensity contrast decay with redshift and as m changes, the behavior of the curves changes.

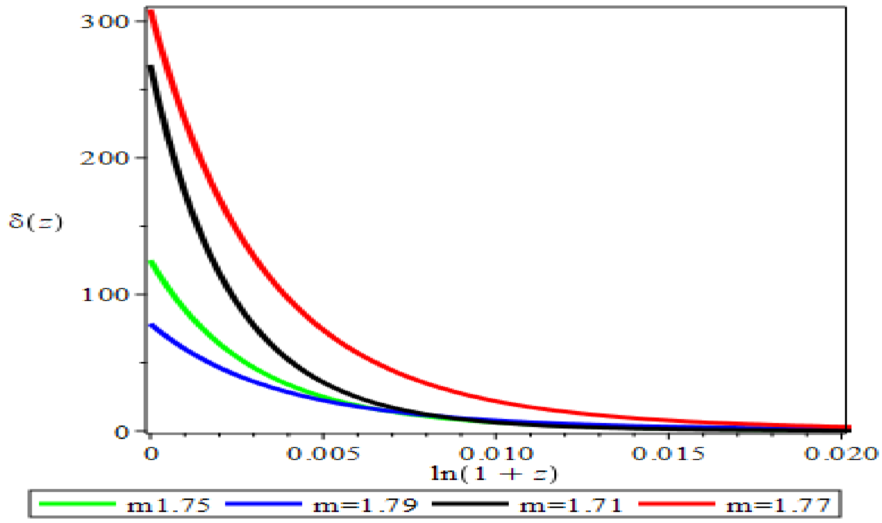

Figure 5: Plot of energy density contrast vs redshift of equations Eq. (53)–(Eq. 58), using $k = 1000$, short wavelength limit. During numerical integration, we considered different constant parameters to see whether there is any effect on the energy density contrast or not whereas $\Delta_s(z_{in} = 4) = 10^{-5}$, $Z(z_{in} = 4) = 10^{-5}$, $\mathcal{G}(z_{in} = 4) = 10^{-5}$, $\mathbf{G}(z_{in} = 4) = 10^{-5}$, $\Delta_{chp}(z_{in} = 4) = 10^{-5}$ were used as initial conditions. From the plots, for different parameter m, we depict that the energy overdensity contrast decay with redshift and as m changes, the behavior of the curves changes.

(1) shows that $\delta(z)$ decay with redshift (z) (normalised to 0 today). Throughout all the plots, we rescaled the $\delta(z)$ to make it readable. By looking at the figures (2) and (3) in the long wavelength mode, the energy density contrast ($\delta(z)$) decays with increase in redshift, but as z increases, the $\delta(z)$ seems to converge as we change the values of parameter m. Changing m affects both the amplitudes and the behavior of the curves. But in the short wavelength mode, as depicted in figures (4) and (5), the energy density contrast decays monotonically with redshift for different values of parameter m and similarly changing the values of m affects the amplitudes of the $\delta(z)$.

4.2 Perturbation equations for modified chaplygin Gas in the context of modified Gauss-Bonnet gravity

Considering the modified chaplygin gas model given by [56, 16]

$$p_{ch} = A\rho - \frac{B}{\rho^{\alpha}}; \tag{62}$$

$$\rho_{chap} = \left[\frac{A}{B+1} + ca^{-3(\alpha+1)(B+1)}\right]^{\frac{1}{\alpha+1}}, \tag{63}$$

where the vector term $a\tilde{\nabla}_a w_{chp}$ provides its scalar part as $a\tilde{\nabla}_a w_{chp} = \frac{B(\alpha+1)}{\rho_{chp}^{\alpha+1}}\Delta_{ch}$. Using this modified chaplygin gas and make time derivative of the scalar gradient variables defined in eq.

(44)–(49), the perturbation equations in redshift space are presented as

$$\Delta_s' = \frac{1}{(1+z)H}\left(2+\frac{2}{(1+w_t)\rho_t}\frac{G\big(-(1+z)H)\big)G'}{\theta^2}\right)Z$$
$$-\frac{1}{(1+z)H}\frac{2}{(1+w_t)}\frac{\rho_s}{\rho_t}\theta\Delta_s+\frac{1}{(1+z)H}\Big(1+\frac{B(\alpha+1)}{\rho_{chp}^{\alpha+1}}\Big)\frac{2}{(1+w_t)\rho_t}w_{chp}\rho_{chp}\Delta_{chp}$$
$$+\frac{2}{(1+w_t)\rho_t}\frac{c\beta(\beta-1)G^{\beta-1}}{\theta}\mathsf{G}-\frac{1}{(1+z)H}\frac{2}{(1+w_t)\rho_t}\Big(\frac{1}{2}(G-c\beta^2G^\beta)(1+z)HG'c\beta(\beta-1)\times$$
$$(\beta-2)G^{\beta-3}-(1+z)HG'c\beta(\beta-1)G^{\beta-4}\Big)\mathcal{G}$$

$$Z' = -\frac{1}{(1+z)H}\Big[-\frac{1}{2}(4\rho_s-(\frac{1}{3}\theta^2+\frac{1}{2}(1+3w_t)\rho_t)\frac{\rho_s}{(1+w_t)\rho_t}-\frac{\rho_s}{(1+w_t)\rho_t}\frac{k^2}{a^2}\Big]\Delta_s$$
$$-\frac{1}{(1+z)H}\Big[\frac{\rho_{ch}\Big(w_{ch}+\frac{B(\alpha+1)}{\rho_{chp}^{\alpha+1}}\Big)}{(1+w_t)\rho_t}\Big(k^2+\frac{\theta^2}{3}+\frac{1}{2}(1+w_t)\rho_t\Big)+\Big(2+3w_{ch}\Big)\rho_{ch}\Big]\Delta_{chp}$$
$$-\frac{1}{(1+z)H}\Big[1-3c\beta(\beta-1)G^{\beta-2}-12H^3b_1c\beta(\beta-1)(\beta-2)(\beta-3)G^{\beta-4}$$
$$+12H\Big(H(b_2c(\beta)(\beta-1)(\beta-2)G^{\beta-3}+\frac{b_3}{b_1}c(\beta)(\beta-1)G^{\beta-2}+b_1^2c(\beta)(\beta-1)(\beta-2)(\beta-3)G^{\beta-4})$$
$$+2H^3c(\beta)(\beta-1)G^{\beta-2}\Big)+(\frac{1}{3}\theta^2+\frac{1}{2}(1+3w_t)\rho_t)\frac{1}{(1+w_t)\rho_t}\Big(\frac{1}{2}(1-c(\beta)G^{\beta-1}-Gc(\beta)G^{\beta-1}$$
$$-Gc(\beta)(\beta-1)G^{\beta-2})+Gb_1c(\beta)(\beta-1)(\beta-2)G^{\beta-3}+b_1c(\beta)(\beta-1)G^{\beta-4}\Big)$$
$$-\frac{1}{(1+w_t)\rho_t}\frac{k^2}{a^2}\Big(\frac{1}{2}(1-c(\beta)G^{\beta-1}-c(\beta)(\beta-1)G^{\beta-1})+b_1c(\beta)(\beta-1)(\beta-2)G^{\beta-2}$$
$$+b_1c(\beta)(\beta-1)G^{\beta-4}\Big)\Big]\mathcal{G}-\frac{1}{(1+z)H}\Big(24b_1c(\beta)(\beta-1)(\beta-2)G^{\beta-3}-12H^3c(\beta)(\beta-1)(\beta-2)G^{\beta-3}$$
$$+(\frac{1}{3}\theta^2+\frac{1}{2}(1+3w_t)\rho_t)\frac{c(\beta)(\beta-1)G^{\beta-1}}{\theta(1+w_t)\rho_t}-\frac{1}{(1+w_t)\rho_t}\frac{k^2}{a^2}\frac{c(\beta)(\beta-1)G^{\beta-1}}{\theta}\Big)\mathbf{G}$$
$$-\frac{1}{(1+z)H}\Big[8H\Big(c(\beta)(\beta-1)G^{\beta-2}b_2+c(\beta)(\beta-1)(\beta-2)G^{\beta-3}b_1^2+3Hc(\beta)G^{\beta-1}$$
$$-\frac{3}{2}c(\beta)(\beta-1)(\beta-2)G^{\beta-3}Hb_1\Big)-\frac{2}{3}\theta-(\frac{1}{3}\theta^2+\frac{1}{2}(1+3w_t)\rho_t)\frac{Gb_1}{\theta^2(1+w_t)\rho_t}$$
$$+\frac{k^2}{a^2(1+w_t)\rho_t}\frac{Gb_1}{\theta^2}\Big]Z \tag{64}$$

$$\mathcal{G}' = -\frac{1}{(1+z)H}\Big(1-\frac{b_1c(\beta)(\beta-1)G^{\beta-1}}{(1+w_t)\rho_t\theta}\Big)\mathsf{G}-\frac{1}{(1+z)H}\frac{b_1^2G}{(1+w_t)\rho_t\theta^2}Z+\frac{1}{(1+z)H}\frac{b_1\rho_s\Delta_s}{(1+w_t)\rho_t}$$
$$-\frac{1}{(1+z)H}\frac{b_1\rho_{ch}}{(1+w_t)\rho_t}\Big(w_{ch}+\frac{B(\alpha+1)}{\rho_{chp}^{\alpha+1}}\Big)\Delta_{ch}+\Big(\frac{1}{2(1+z)H}\frac{b_1}{(1+w_t)\rho_t}\Big(c(\beta)G^{\beta-1}$$
$$+c(\beta)(\beta-1)G^{\beta-1}-1\Big)+\frac{1}{2(1+z)H}\frac{b_1^2}{(1+w_t)\rho_t}\Big(c(\beta)(\beta-1)G^{\beta-1}+\frac{c(\beta)(\beta-1)G^{\beta-2}}{\theta^2}\Big)\Big)\mathcal{G} \tag{65}$$

$$
\begin{aligned}
\mathsf{G}' &= -\frac{1}{(1+z)H}\Big(\frac{b_3}{b_1} - \frac{b_1 c(\beta)(\beta-1)G^{\beta-1}}{(1+w_t)\rho_t\theta}\Big)\mathsf{G} + \Big[\frac{1}{(1+z)H}\frac{b_2 b_1 G}{(1+w_t)\rho_t\theta^2}\Big]Z \\
&+\Big[\frac{1}{(1+z)H}\frac{b_2}{(1+w_t)\rho_t}\rho_s\Big]\Delta_s - \Big[\frac{1}{(1+z)H}\frac{b_2\rho_{ch}}{(1+w_t)\rho_t}\Big(w_{ch} + \frac{B(\alpha+1)}{\rho_{chp}^{\alpha+1}}\Big)\Big]\Delta_{ch} \\
&-\frac{1}{(1+z)H}\Big[\frac{b_2}{2(1+w_t)\rho_t}(c(\beta)G^{\beta-1} + c(\beta)(\beta-1)G^{\beta-1} - 1) - \frac{b_2 b_1}{(1+w_t)\rho_t}(c(\beta)(\beta-1)G^{\beta-1} \\
&+\frac{c(\beta)(\beta-1)G^{\beta-2}}{\theta^2})\Big]\mathcal{G} \qquad (66)
\end{aligned}
$$

$$
\begin{aligned}
\Delta'_G &= -\frac{1}{(1+z)H}\Big[-\frac{4H\theta}{\rho_G}\Big(2Hb_1c(\beta)(\beta-1)(\beta-2)G^{\beta-3} + (2c_1 - 2H^2)c(\beta)(\beta-1)G^{\beta-2}\Big) \\
&+\theta\Big(4H^2c(\beta)(\beta-1)G^{\beta-2}b_2 + 4H(2c_1 - H^2)c(\beta)(\beta-1)G^{\beta-2}b_1\Big)\Big(\frac{c(\beta)(\beta-1)G^{\beta-1}}{\theta(1+w_t)\rho_t\rho_G}\Big)\Big]\mathsf{G} \\
&-\frac{1}{(1+z)H}\Big[4H\Big(H(b_2c(\beta)(\beta-1)(\beta-2)G^{\beta-3} + \frac{c(\beta)(\beta-1)G^{\beta-2}b_2}{b_2} + b_2^2c(\beta)(\beta-1)(\beta-2)G^{\beta-3}) \\
&+(2c_1 - H^2)c(\beta)(\beta-1)G^{\beta-2}\Big) + \theta\Big(4H^2(c(\beta)(\beta-1)G^{\beta-2}b_2 + c(\beta)(\beta-1)(\beta-2)G^{\beta-3}b_1^2)) \\
&+4H(2c_1 - H^2)c(\beta)(\beta-1)G^{\beta-2}b_1\Big(\frac{\frac{1}{2} + b_1c(\beta)(\beta-1)G^{\beta-1} + \frac{b_1c(\beta)(\beta-1)(\beta-2)G^{\beta-3}}{\theta^2}}{(1+w_t)\rho_t\rho_G}\Big)\Big]\mathcal{G} + \\
&-\frac{1}{3((1+z)H)\rho_G}\Big[\Big(2H(c(\beta)(\beta-1)G^{\beta-2}b_2 + c(\beta)(\beta-1)(\beta-2)G^{\beta-3}b_1^2) - 8Hc(\beta)(\beta-1)G^{\beta-2}\times \\
&b_1(\frac{G}{12H^3} + 3H) + (2c_1 - H^2)c(\beta)(\beta-1)G^{\beta-2}b_1 - 3\Big(4H^2(c(\beta)(\beta-1)G^{\beta-2}b_2 + c(\beta)(\beta-1)\times \\
&(\beta-2)G^{\beta-3}b_1^2) + 4H(2c_1 - H^2)c(\beta)(\beta-1)G^{\beta-2}b_1\Big) + \theta(4H^2(c(\beta)(\beta-1)G^{\beta-2}b_2 \\
&+c(\beta)(\beta-1)(\beta-2)G^{\beta-3}b_1^2) - 4H(2c_1 - H^2)c(\beta)(\beta-1)G^{\beta-2}b_1)(\frac{Gb_1\theta^2}{(1+w_t)\rho_t\rho_G})\Big) \\
&+3\theta(4H^2(c(\beta)(\beta-1)G^{\beta-2}b_2 + c(\beta)(\beta-1)(\beta-2)G^{\beta-3}b_1^2) + 4H(2c_1 - H^2)c(\beta)(\beta-1)G^{\beta-2}b_1)\times \\
&\Big(\frac{(1-(2+\beta)c(\beta)G^{\beta}b_1}{\theta^2(1+w_t)\rho_t}\Big)\Big]Z - \frac{3}{(1+z)\rho_G}\Big(4H^2(c(\beta)(\beta-1)G^{\beta-2}b_2 + c(\beta)(\beta-1)(\beta-2)G^{\beta-3}b_1^2) \\
&+4H(2c_1 - H^2)f''b_1\Big)\Delta_G - \frac{3}{(1+z)}\Big(-4H^2(c(\beta)(\beta-1)G^{\beta-2}b_2 + c(\beta)(\beta-1)(\beta-2)G^{\beta-3}b_1^2) \\
&+4H(2c_1 - H^2)c(\beta)(\beta-1)G^{\beta-2}b_1\Big)\frac{\rho_s(1 - c(\beta)G^{\beta-1} - c(\beta)(\beta-1)G^{\beta-1})}{(1 + w_t\rho_t\rho_G)}\Delta_s \\
&+\frac{3}{(1+z)}\Big(4H^2(c(\beta)(\beta-1)G^{\beta-2}b_2 + c(\beta)(\beta-1)(\beta-2)G^{\beta-3}b_1^2) \\
&+4H(2c_1 - H^2)c(\beta)(\beta-1)G^{\beta-2}b_1\Big)\Big(\frac{w_{ch}\rho_{ch}}{(1+w_t)\rho_t\rho_G}\Big)\Big(\frac{B(\alpha+1)}{\rho_{chp}^{\alpha+1}}\Big)\Delta_{chp} \qquad (67)
\end{aligned}
$$

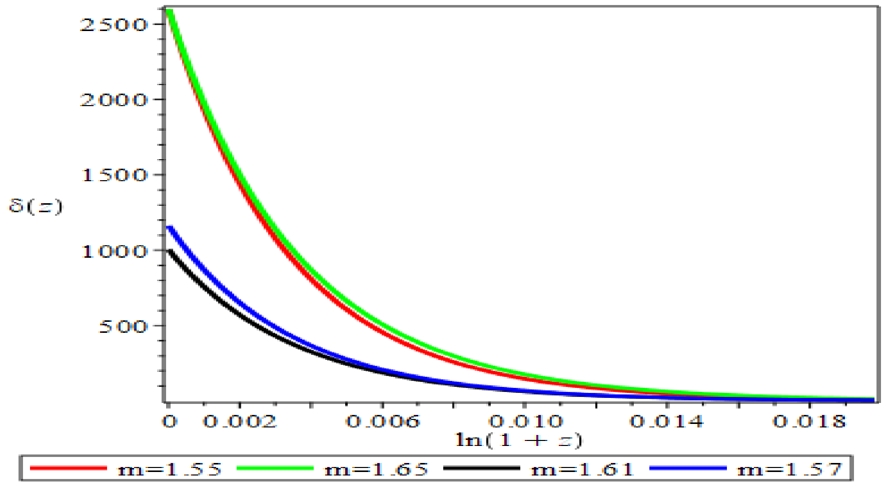

Figure 6: Plot of energy density contrast vs redshift of equations Eq. (64)–(Eq. 68), using $k = 0.000001$, long wavelength limit. During numerical integration, we considered different constant parameters to see whether there is any effect on the energy density contrast or not whereas $\Delta_s(z_{in} = 4) = 10^{-5}$, $Z(z_{in} = 4) = 10^{-5}$, $\mathcal{G}(z_{in} = 4) = 10^{-5}$, $\mathbf{G}(z_{in} = 4) = 10^{-5}$, $\Delta_{chp}(z_{in} = 4) = 10^{-5}$ were used as initial conditions. From the plots, for different parameter m, we depict that the energy overdensity contrast decay with redshift and as m changes, the behavior of the curves changes.

$$\Delta^{'}_{ch} = \frac{1}{(1+z)H}[1+\frac{Gb_1}{\theta(1+w_t)\rho_t}](1+w_{ch})Z - \frac{1}{(1+z)H}\frac{\theta(1+w_{ch})}{(1+w_t)\rho_t}\rho_s\Delta_s$$
$$-\frac{3}{(1+z)}\Big[(1+\rho_{ch})\frac{(1+w_{ch})}{(1+w_t)\rho_t}w_{ch}\rho_{ch} - \Big(1+\frac{B(\alpha+1)}{\rho_{chp}^{\alpha+1}}\Big)\theta\Big]\Delta_{ch}$$
$$-\frac{\theta(1+w_{ch})}{(1+z)(1+w_t)H\rho_t}\Big[\frac{1}{2}(1-c(\beta)G^{\beta-1} - c(\beta)(\beta-1)G^{\beta-1}) + b_1c(\beta)(\beta-1)G^{\beta-1}$$
$$+\frac{b_1c(\beta)(\beta-1)(\beta-2)G^{\beta-3}}{\theta^2}\Big]\mathcal{G} - \frac{\theta(1+w_{ch})c(\beta)(\beta-1)G^{\beta-1}}{(1+z)(1+w_t)H\rho_t}\mathsf{G}\,. \tag{68}$$

The equations eq. (64–68) represent the evolution of the energy density of the stiff fluid, the volume expansion, the Gauss-Bonnet fluid, Gauss-Bonnet momentum, the energy density resulting from the Gauss-Bonnet fluid and the energy density of the modified chaplygin gas, respectively. The perturbation equations in redshift space presented in this work (eq. (64)–(68)) are coupled system of first-order ordinary differential equations for the density fluctuations of stiff-, modified-chaplygin gas and Gauss-Bonnet fluids, which are more complicated to find the analytical solutions. We have considered short wavelength ($\frac{k^2}{a^2H^2} \gg 1$) and long wavelength ($\frac{k^2}{a^2H^2} \ll 1$) limits of the perturbation to numerically integrate the perturbation equations and to analyse the large scale structure implications of the numerical results using different initial conditions. In the following, by considering that the universe is mainly dominated by stiff-modified chaplygin gas-Gauss-Bonnet fluids mixture, the numerical results are presented in fig. (6) and fig. (7) for long wavelength modes whereas figs. (8) and (9) contain the results of the perturbation equations in the short wavelength mode. During numerical integration, we considered different constant parameters to see whether there is any effect on the energy density contrast or not, whereas $\Delta_s(z_{in} = 4) = 10^{-5}$, $Z(z_{in} = 4) = 10^{-5}$, $\mathcal{G}(z_{in} = 4) = 10^{-5}$,

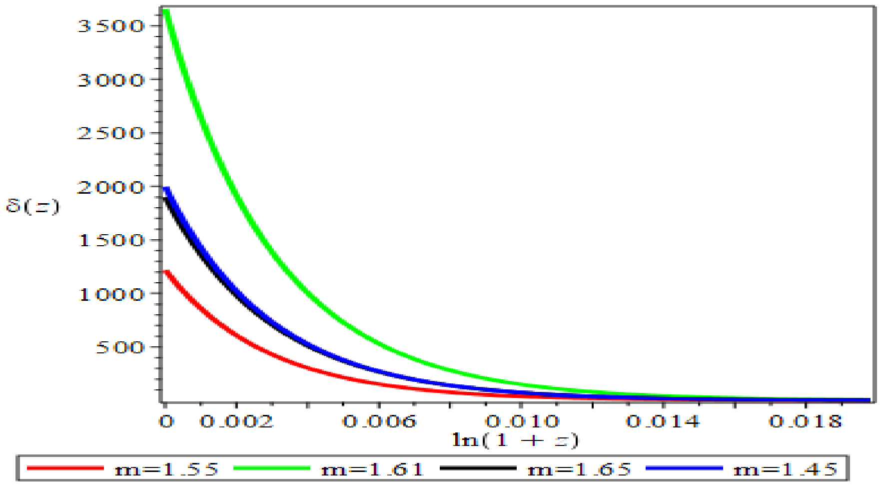

Figure 7: Plot of energy density contrast vs redshift of equations Eq. (64)–(Eq. 68), using $k = 0.01$, long wavelength limit. During numerical integration, we considered different constant parameters to see whether there is any effect on the energy density contrast or not whereas $\Delta_s(z_{in} = 4) = 10^{-5}$, $Z(z_{in} = 4) = 10^{-5}$, $\mathcal{G}(z_{in} = 4) = 10^{-5}$, $\mathbf{G}(z_{in} = 4) = 10^{-5}$, $\Delta_{chp}(z_{in} = 4) = 10^{-5}$ were used as initial conditions. From the plots, for different parameter m, we depict that the energy overdensity contrast decay with redshift and as m changes, the behavior of the curves changes.

$\mathbf{G}(z_{in} = 4) = 10^{-5}$, $\Delta_{chp}(z_{in} = 4) = 10^{-5}$ were used as initial conditions. From the plots, for different parameter m, we depict that the energy overdensity contrast decay with redshift and as m changes, the behavior of the curves changes. By looking at the figures (6) and (7) in the long wavelength mode, the energy density contrast ($\delta(z)$) decays with redshift. Changing m affects both the amplitudes and does not affect the behavior of the curves. In the short wavelength mode, as can be depicted in fig. (8) and fig. (9), the energy density contrast decays with redshift for different values of parameter m and similarly changing the values of m affects the amplitudes of the $\delta(z)$.

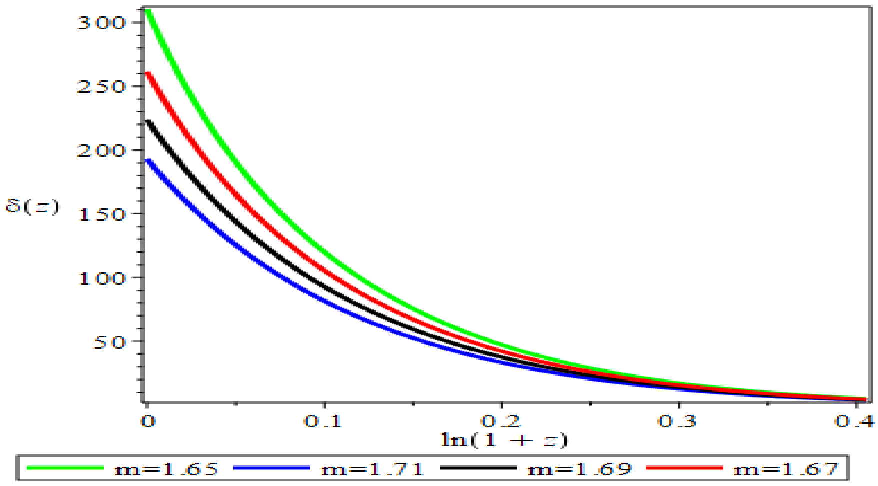

Figure 8: Plot of energy density contrast vs redshift of equations Eq. (64)–(Eq. 68), using $k = 100$, short wavelength limit. During numerical integration, we considered different constant parameters to see whether there is any effect on the energy density contrast or not whereas $\Delta_s(z_{in} = 4) = 10^{-5}$, $Z(z_{in} = 4) = 10^{-5}$, $\mathcal{G}(z_{in} = 4) = 10^{-5}$, $\mathbf{G}(z_{in} = 4) = 10^{-5}$, $\Delta_{chp}(z_{in} = 4) = 10^{-5}$ were used as initial conditions. From the plots, for different parameter m, we depict that the energy overdensity contrast decay with redshift and as m changes, the behavior of the curves changes.

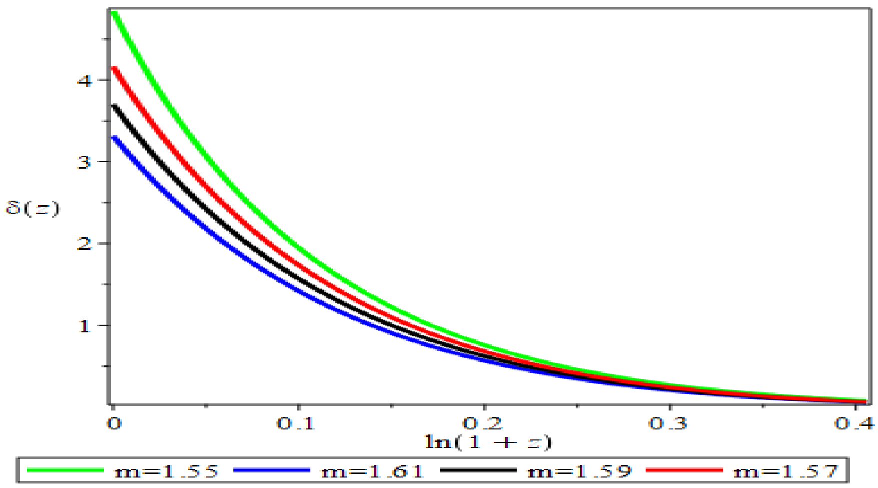

Figure 9: Plot of energy density contrast vs redshift of equations Eq. (64)–(Eq. 68), using $k = 1000$, short wavelength limit. During numerical integration, we considered different constant parameters to see whether there is any effect on the energy density contrast or not whereas $\Delta_s(z_{in} = 4) = 10^{-5}$, $Z(z_{in} = 4) = 10^{-5}$, $\mathcal{G}(z_{in} = 4) = 10^{-5}$, $\mathbf{G}(z_{in} = 4) = 10^{-5}$, $\Delta_{chp}(z_{in} = 4) = 10^{-5}$ were used as initial conditions. From the plots, for different parameter m, we depict that the energy overdensity contrast decay with redshift and as m changes, the behavior of the curves changes.

Rwanda Journal of Engineering, Science, Technology and Environment, Volume 7, Issue 1, Month 2025
eISSN: 2617-233X — print ISSN: 2617-2321

5 Conclusion

In this work, the treatment of the $1+3$ covariant perturbations is made in the context of stiff-Gauss-Bonnet fluids mixture using two different forms of chaplygin gas model, namely generalised modified chaplygin gas and modified chaplygin gas. This study aimed to investigate the validity and broader implications of the $f(G)$ gravity with a focus on the multifluid system. The theoretical foundation of this fluids mixture was explored in section (1) and expanded in sec. (2), where the contribution of stiff fluid, generalised modified chaplygin gas and Gauss-Bonnet fluid was integrated into the effective energy density and pressure. Using scalar decomposition, harmonic decomposition methods together with redshift transformation technique presented in eqs. (23)–(25), the time derivative of eqs. (44)–(49), incorporating spatial gradient variables of the stiff fluid and the volume expansion and Gauge-Invariant variables defining the fluctuations of the energy density and momentum of the Gauss-Bonnet and chaplygin gas model, yields the perturbation equations of the stiff fluid-chaplygin gas-Gauss-Bonnet fluid mixture in redshift space presented in eqs. (53)–(58) for the generalised modified chaplygin gas model and eqs. (64)–(68) for the modified chaplygin gas. In order to solve the already obtained perturbation equations, the energy density contrast ($\delta(z)$) was formulated to understand the formation and evolution of large scale structures in the Universe. The analysis wa conducted in both long and short wavelength modes and presented the numerical results by considering three different cases, namely: the case where the universe is only dominated by the stiff fluid thereafter GR or ΛCDM model, the case where the evolution of the universe is driven by the fluid mixture of stiff fluid-generalised modified chaplygin gas and the mixture of stiff fluid-modified chaplygin gas in the context of modified Gauss-Bonnet gravity. The results of the stiff fluid case is presented in fig. (1), those of stiff fluid-generalised modified chaplygin gas mixture are presented in figs. (2) and (3) for long wavelength modes and in figs. (4) and (5) for short wavelength mode, whereas the results orginating from the mixture of stiff fluid-modified chaplygin gas are presented in figs. (6) and (7) for long wavelength modes and in figs. (8) and (9) for short wavelength mode. Following the definition of the $\delta(z)$, firstly without considering the chaplygin gas and Gauss-Bonnet fluid, we note that from fig. (1), $\delta(z)$ decays monotonically with redshift. In terms of decaying of $\delta(z)$, the stiff fluid-modified chaplygin gas mixture performed the best for every values of parameter m changed in both long and short wavelength modes, but the stiff fluid-generalised modified chaplygin gas mixture do not decay monotonically as the case of stiff fluid consideration as m changes, especially in the long wavelength mode. Over all, from the numerical results, as far as large scale structure formation is concerned, we note that there is no real difference on the effects of using different chaplygin gas models in short wavelength mode while in the long wavelength mode, only the stiff fluid-generalised modified chaplygin gas mixture shows a slightly small difference in the behavior of the curves. Furthermore, the fluid mixtures considered may be considered as viable models for studying the formation and evolution of large scale structures in the Universe relative to GR model. Interestingly, we note that the stiff fluid-modified chaplygin gas mixture in the context of $f(G)$ gravity presents a faster grow of structures (higher amplitude of perturbations) than predicted in the GR or ΛCDM model, which requires further research and testing against observational data using different toy $f(G)$ models. This will be done elsewhere.

https://dx.doi.org/10.4314/rjeste.v7i1.1

Acknowledgments

The authors acknowledge the financial support from UR-SIDA Grant No. DVC-AAR 506/2022. AM acknowledges the support in part from Swedish International Development Agency (SIDA) through International Science Program (ISP) of the Uppsala University to the East African Astronomical Research Network (EAARN), Grant No. AFRO:05. AM also acknowledges the hospitality of the department of Physics of the University of Rwanda, where part of this work was conceptualized and completed.

References

[1] Terry P Walker, Gary Steigman, David N Schramm, Keith A Olive, and Ho-Shik Kang. Primordial nucleosynthesis redux. *Astrophysical Journal, Part 1 (ISSN 0004-637X), vol. 376, July 20, 1991, p. 51-69.*, 376:51–69, 1991.

[2] Eiichiro Komatsu, J Dunkley, MR Nolta, CL Bennett, B Gold, G Hinshaw, N Jarosik, D Larson, M Limon, LEA Page, et al. Five-year wilkinson microwave anisotropy probe* observations: cosmological interpretation. *The Astrophysical Journal Supplement Series*, 180(2):330, 2009.

[3] Alexandre Refregier. Weak gravitational lensing by large-scale structure. *Annual Review of Astronomy and Astrophysics*, 41(1):645–668, 2003.

[4] J Anthony Tyson, Greg P Kochanski, and Ian P Dell'Antonio. Detailed mass map of cl 0024+ 1654 from strong lensing. *The Astrophysical Journal*, 498(2):L107, 1998.

[5] SW Allen, RW Schmidt, AC Fabian, and H Ebeling. Cosmological constraints from the local x-ray luminosity function of the most x-ray-luminous galaxy clusters. *Monthly Notices of the Royal Astronomical Society*, 342(1):287–298, 2003.

[6] Vera C Rubin, W Kent Ford Jr, and Norbert Thonnard. Rotational properties of 21 sc galaxies with a large range of luminosities and radii, from ngc 4605/r= 4kpc/to ugc 2885/r= 122 kpc. *Astrophysical Journal, Part 1, vol. 238, June 1, 1980, p. 471-487.*, 238:471–487, 1980.

[7] Sourish Dutta and Robert J Scherrer. Big bang nucleosynthesis with a stiff fluid. *Physical Review D-Particles, Fields, Gravitation, and Cosmology*, 82(8):083501, 2010.

[8] Malcolm Hicken, W Michael Wood-Vasey, Stephane Blondin, Peter Challis, Saurabh Jha, Patrick L Kelly, Armin Rest, and Robert P Kirshner. Improved dark energy constraints from 100 new cfa supernova type ia light curves. *The Astrophysical Journal*, 700(2):1097, 2009.

[9] Will J Percival, Beth A Reid, Daniel J Eisenstein, Neta A Bahcall, Tamas Budavari, Joshua A Frieman, Masataka Fukugita, James E Gunn, Željko Ivezić, Gillian R Knapp, et al. Baryon acoustic oscillations in the sloan digital sky survey data release 7 galaxy sample. *Monthly Notices of the Royal Astronomical Society*, 401(4):2148–2168, 2010.

[10] Lado Samushia and Bharat Ratra. Constraining dark energy with gamma-ray bursts. *The Astrophysical Journal*, 714(2):1347, 2010.

[11] Vittorio Gorini, Alexander Kamenshchik, Ugo Moschella, and Vincent Pasquier. The chaplygin gas as a model for dark energy. In *The Tenth Marcel Grossmann Meeting: On Recent Developments in Theoretical and Experimental General Relativity, Gravitation and Relativistic Field Theories (In 3 Volumes)*, pages 840–859. World Scientific, 2005.

[12] M Conceicao Bento, Orfeu Bertolami, and Anjan A Sen. Generalized chaplygin gas, accelerated expansion, and dark-energy-matter unification. *Physical Review D*, 66(4):043507, 2002.

[13] Maria da Conceicao Bento, O Bertolami, and AA Sen. Generalized chaplygin gas and cosmic microwave background radiation constraints. *Physical Review D*, 67(6):063003, 2003.

[14] YA Maye. *Elmardi. Topics in Relativistic Cosmology.* PhD thesis, PhD thesis, 2018.

[15] Shambel Sahlu, Heba Sami, Renier Hough, Maye Elmardi, Anna-Mia Swart, and Amare Abebe. Confronting the chaplygin gas with data: Background and perturbed cosmic dynamics. *International Journal of Modern Physics D*, 32(13):2350090, 2023.

[16] Renier Hough, Shambel Sahlu, Heba Sami, Maye Elmardi, Anna-Mia Swart, and Amare Abebe. Confronting the chaplygin gas with data: background and perturbed cosmic dynamics. *arXiv preprint arXiv:2112.11695*, 2021.

[17] Ya B Zeldovich. Survey of modern cosmology. In *Advances in astronomy and astrophysics*, volume 3, pages 241–379. Elsevier, 1965.

[18] K Rajagopalan Nair and Titus K Mathew. A model of the late universe with viscous zel'ldovich fluid and decaying vacuum. *Astrophysics and Space Science*, 363:1–10, 2018.

[19] Daniel JH Chung, Lisa L Everett, and Konstantin T Matchev. Inflationary cosmology connecting dark energy and dark matter. *Physical Review D—Particles, Fields, Gravitation, and Cosmology*, 76(10):103530, 2007.

[20] Rainer Stiele, Tillmann Boeckel, and Jürgen Schaffner-Bielich. Cosmological implications of a dark matter self-interaction energy density. *Physical Review D—Particles, Fields, Gravitation, and Cosmology*, 81(12):123513, 2010.

[21] Gianluca Calcagni. Cosmology of the lifshitz universe. *Journal of High Energy Physics*, 2009(09):112, 2009.

[22] Elias Kiritsis and Georgios Kofinas. Hořava–lifshitz cosmology. *Nuclear Physics B*, 821(3):467–480, 2009.

[23] Amna Ali, Sourish Dutta, Emmanuel N Saridakis, and Anjan A Sen. Hořava-lifshitz cosmology with generalized chaplygin gas. *General Relativity and Gravitation*, 44:657–683, 2012.

[24] Leonardo Fernández-Jambrina and Luis Manuel González-Romero. A wide family of singularity-free cosmological models. *Physical Review D*, 66(2):024027, 2002.

[25] Naresh Dadhich and LK Patel. Uniqueness of the non-singular family and characterisation of cosmological models. *arXiv preprint gr-qc/9406034*, 1994.

[26] L Fernández-Jambrinaa. Singularity-free cylindrical cosmological model. *Classical and Quantum Gravity*, 14(12):3407, 1997.

[27] C Pallis. Kination-dominated reheating and cold dark matter abundance. *Nuclear Physics B*, 751(1-2):129–159, 2006.

[28] Fiorenza Donato, Nicolao Fornengo, and Mia Schelke. Additional bounds on the pre-big-bang-nucleosynthesis expansion by means of γ-rays from the galactic centre. *Journal of Cosmology and Astroparticle Physics*, 2007(03):021, 2007.

[29] Eduard Massó and Francesc Rota. Primordial nucleosynthesis as a test of the friedmann equation in the early universe. *Physical Review D*, 68(12):123504, 2003.

[30] Joseph Ntahompagaze, Amare Abebe, and Manasse Mbonye. On f (r) gravity in scalar–tensor theories. *International Journal of Geometric Methods in Modern Physics*, 14(07):1750107, 2017.

[31] Heba Sami, Neo Namane, Joseph Ntahompagaze, Maye Elmardi, and Amare Abebe. Reconstructing f (r) gravity from a chaplygin scalar field in de sitter spacetimes. *International Journal of Geometric Methods in Modern Physics*, 15(02):1850027, 2018.

[32] Salvatore Capozziello, Carlo Alberto Mantica, and Luca Guido Molinari. Cosmological perfect-fluids in $f(R)$ gravity. *International Journal of Geometric Methods in Modern Physics*, 16(01):1950008, 2019.

[33] Baojiu Li, John D Barrow, and David F Mota. Cosmology of modified gauss-bonnet gravity. *Physical Review D-Particles, Fields, Gravitation, and Cosmology*, 76(4):044027, 2007.

[34] Eugeny Babichev and David Langlois. Relativistic stars in $f(R)$ and scalar-tensor theories. *Physical Review D-Particles, Fields, Gravitation, and Cosmology*, 81(12):124051, 2010.

[35] Kazuharu Bamba, Sergei D Odintsov, Lorenzo Sebastiani, and Sergio Zerbini. Finite-time future singularities in modified gauss–bonnet and $f(R, G)$ gravity and singularity avoidance. *The European Physical Journal C*, 67:295–310, 2010.

[36] Alexander D Dolgov and Masahiro Kawasaki. Can modified gravity explain accelerated cosmic expansion? *Physics Letters B*, 573:1–4, 2003.

[37] Shin'ichi Nojiri, Sergei D Odintsov, and Petr V Tretyakov. From inflation to dark energy in the non-minimal modified gravity. *Progress of Theoretical Physics Supplement*, 172:81–89, 2008.

[38] Yusaku Ito, Shin'ichi Nojiri, and Sergei D Odintsov. Stability of accelerating cosmology in two scalar-tensor theory: little rip versus de sitter. *Entropy*, 14(8):1578–1605, 2012.

[39] Shin'ichi Nojiri, Sergei D Odintsov, Vasilis K Oikonomou, and Arkady A Popov. Ghost-free f (r, g) gravity. *Nuclear Physics B*, 973:115617, 2021.

[40] Shin'ichi Nojiri and Sergei D Odintsov. The dark universe future and singularities: The account of thermal and quantum effects. *Physics of the Dark Universe*, 30:100695, 2020.

[41] VK Oikonomou and FP Fronimos. Non-minimally coupled einstein–gauss–bonnet gravity with massless gravitons: the constant-roll case. *The European Physical Journal Plus*, 135(11):917, 2020.

[42] Sergei D Odintsov, Vasilis K Oikonomou, and FP Fronimos. Rectifying einstein-gauss-bonnet inflation in view of gw170817. *Nuclear Physics B*, 958:115135, 2020.

[43] VK Oikonomou. A refined einstein–gauss–bonnet inflationary theoretical framework. *Classical and Quantum Gravity*, 38(19):195025, 2021.

[44] FP Fronimos and SA Venikoudis. Inflation with exotic kinetic terms in einstein–chern–simons gravity. *International Journal of Modern Physics A*, 36(30):2150229, 2021.

[45] Albert Munyeshyaka, Joseph Ntahompagaze, Tom Mutabazi, and Manasse Mbonye. On covariant perturbations with scalar field in modified gauss–bonnet gravity. *The European Physical Journal C*, 84(1):51, 2024.

[46] Albert Munyeshyaka, Praveen Kumar Dhankar, and Joseph Ntahompagaze. Perturbations with bulk viscosity in modified chaplygin gas cosmology. *Available at SSRN 4777710*.

[47] Fidele Twagirayezu, Abraham Ayirwanda, Albert Munyeshyaka, Solange Mukeshimana, Joseph Ntahompagaze, and Leon Fidele Ruganzu Uwimbabazi. On chaplygin models in $f(G)$ gravity. *arXiv preprint arXiv:2305.19711*, 2023.

[48] Evgenii Mikhailovich Lifshitz. On the gravitational stability of the expanding universe. *J. Phys.*, 10:116–129, 1946.

[49] James M Bardeen. Gauge-invariant cosmological perturbations. *Physical Review D*, 22(8):1882, 1980.

[50] Hideo Kodama and Misao Sasaki. Cosmological perturbation theory. *Progress of Theoretical Physics Supplement*, 78:1–166, 1984.

[51] Jürgen Ehlers. Beiträge zur relativistischen mechanik kontinuierlicher medien. In *Abhandlungen der Mathematisch-Naturwissenschaftlichen Klasse*, pages 793–836. 1961.

[52] Stephen W Hawking. Perturbations of an expanding universe. *Astrophysical Journal, vol. 145, p. 544*, 145:544, 1966.

[53] DW Olson. Density perturbations in cosmological models. *Physical Review D*, 14(2):327, 1976.

[54] George FR Ellis and Marco Bruni. Covariant and gauge-invariant approach to cosmological density fluctuations. *Physical Review D*, 40(6):1804, 1989.

[55] Amare Abebe, Alnadhief HA Alfedeel, Değer Sofuoğlu, Eltegani I Hassan, and Rishi Kumar Tiwari. Perturbations in bianchi-v spacetimes with varying λ, g and viscous fluids. *Universe*, 9(2):61, 2023.

[56] Maye Elmardi, Amare Abebe, and Abiy Tekola. Chaplygin-gas solutions of $f(R)$ gravity. *International Journal of Geometric Methods in Modern Physics*, 13(10):1650120, 2016.

[57] Shambel Sahlu, Joseph Ntahompagaze, Maye Elmardi, and Amare Abebe. The chaplygin gas as a model for modified teleparallel gravity? *The European Physical Journal C*, 79(9):1–31, 2019.

[58] Shambel Sahlu, Heba Sami, Anna-Mia Swart, Thato Tsabone, Maye Elmardi, and Amare Abebe. Perturbations in a chaplygin gas cosmology. *arXiv preprint arXiv:2010.05173*, 2020.

[59] Edmund J Copeland, Mohammad Sami, and Shinji Tsujikawa. Dynamics of dark energy. *International Journal of Modern Physics D*, 15(11):1753–1935, 2006.

[60] Nadiezhda Montelongo Garcia, Tiberiu Harko, Francisco SN Lobo, and José P Mimoso. Energy conditions in modified gauss-bonnet gravity. *Physical Review D-Particles, Fields, Gravitation, and Cosmology*, 83(10):104032, 2011.

[61] Albert Munyeshyaka, Joseph Ntahompagaze, Tom Mutabazi, Manasse R Mbonye, Abraham Ayirwanda, Fidele Twagirayezu, and Amare Abebe. Perturbations in the interacting vacuum. *International Journal of Geometric Methods in Modern Physics*, 20(03):2350047, 2023.

[62] Shambel Sahlu, Joseph Ntahompagaze, Amare Abebe, Álvaro de la Cruz-Dombriz, and David F Mota. Scalar perturbations in $f(T)$ gravity using the 1+ 3 covariant approach. *The European Physical Journal C*, 80(5):422, 2020.

[63] Chris Clarkson. Covariant approach for perturbations of rotationally symmetric spacetimes. *Physical Review D-Particles, Fields, Gravitation, and Cosmology*, 76(10):104034, 2007.

[64] Joseph Ntahompagaze, Amare Abebe, and Manasse Mbonye. A study of perturbations in scalar–tensor theory using 1+ 3 covariant approach. *International Journal of Modern Physics D*, 27(03):1850033, 2018.

[65] Joseph Ntahompagaze, Shambel Sahlu, Amare Abebe, and Manasse R Mbonye. On multifluid perturbations in scalar–tensor cosmology. *International Journal of Modern Physics D*, 29(16):2050120, 2020.

[66] Amare Abebe, Mohamed Abdelwahab, Alvaro De la Cruz-Dombriz, and Peter KS Dunsby. Covariant gauge-invariant perturbations in multifluid $f(R)$ gravity. *Classical and quantum gravity*, 29(13):135011, 2012.